Macromolecules
ARTICLE

Macromolecules **2010**, *43*, 1551–1555 **1551**
DOI: 10.1021/ma902509y

Nondestructive Probing of Mechanical Anisotropy in Polyimide Films on Nanoscale

N. Gomopoulos,[†] G. Saini,[‡] M. Efremov,*[,∥] P. F. Nealey,[∥] K. Nelson,[‡] and G. Fytas*[,†,§,⊥]

[†]*Max Planck Institute for Polymer Research Ackermannweg 10, 55128 Mainz, Germany,* [‡]*Department of Chemistry, and* [§]*Department of Materials Science and Engineering, Massachusetts Institute of Technology, Cambridge, Massachusetts 02139,* [∥]*Department of Chemical and Biological Engineering, University of Wisconsin-Madison, Wisconsin 53706, and* [⊥]*Department of Materials Science University of Crete and F.O.R.T.H 77110, Heraklion, Greece*

Received November 12, 2009; Revised Manuscript Received December 28, 2009

ABSTRACT: The present work demonstrates the first application of Brillouin light scattering to probe elastic excitations in highly anisotropic polymer thin films. Both the in-plane and out-of-plane longitudinal and shear moduli of poly(biphenyl dianhydride-*p*-phenylenediamine) (BPDA-PDA) polyimide were accessed by utilizing the transmission and reflection scattering geometries [*Macromolecules* **2007**, *40*, 7283; **2009**, *42*, 7164]. A series of thin BPDA-PDA polyimide coatings on transparent substrates with thickness in the range of 0.1−20 μm were explored, and no noticeable trend in elastic properties and mechanical anisotropy with thickness has been found, in conformity with earlier results. The earlier studies were restricted to thick films (>1.5 μm) and to the in-plane moduli.

Introduction

Nondestructive probing of elastic properties has become a state-of-art approach in thin film research and applications because of recent advances and growing popularity of acousto-optical methods, in particular, Brillouin light scattering (BLS)[1,2] and impulsive stimulated thermal scattering (ISTS).[3] The ability of these methods to measure elastic constants along different directions can hardly be overestimated for anisotropic film samples, frequently found in practical applications (stretched packing films, for example). Mechanical anisotropy correlates with preferred orientation of structural units in tested material; this correlation is extensively used to analyze the effect of processing conditions on structure and mechanical stability of films.[4−6] It should be noted that the other parameter widely used for anisotropy characterization is optical birefringence, which shows much less magnitude than elastic moduli ratio in some polymer films.[5,6]

Until now, progress in nondestructive testing of elastic properties is limited mainly to free-standing films. The presence of complex acoustic modes in spectra of supported films and coatings makes the data difficult to analyze.[3,7] In a few studies of anisotropic coatings by acousto-optical methods, ISTS is utilized and the films under investigation are substantially thicker than 1 μm.[8,9] For the important class of submicrometer coatings (extensively used in microlithography), probing of elastic constants is performed on films with either known or assumed isotropy[2,10−15] and often limited to one specific direction.[2,14,15]

Here we report the first systematic study of mechanical anisotropy in highly anisotropic supported films in the 0.1−20 μm thickness range made by the BLS technique. Polyimide coatings chosen for this investigation are well known for their directionally dependent properties; both free-standing and supported polyimide films are often used as model polymer layers[16] with strong uniaxial anisotropy of optical,[17−20] mechanical,[8,9,21−23] and thermal[24,25] characteristics. Moreover, outstanding mechanical properties, high dimensional and thermal stability, low thermal expansion, and low dielectric constant of polyimide make it the material of choice for protective coatings[26] and for interlayer dielectrics and passivation layers in microelectronic industry.[27] Aromatic polyimides are the most successful and widely used polymeric high-performance materials for space applications.[28] High technological importance of polyimide coatings calls for adequate directionally dependent characterization tools, and thus application of BLS to these objects is practically sound.

Recent advances in BLS technique make possible independent probing of in-plane and out-of-plane elastic moduli of submicrometer coatings. Whereas in-plane parameters can be determined by utilizing typical transmission scattering geometry, the reflection configuration opens the way to probe standing elastic excitations confined normal to the surface. A combination of these two approaches makes possible adequate and nondestructive characterization of mechanical anisotropy in polymer coatings of micrometer and submicrometer thickness range.

Experimental Section

Sample Preparation. Several types of transparent substrates were used. Type 1, 25 mm diameter microscope cover slides made by optical borosilicate glass (Fisher brand 25CIR1D) were used for <500 nm thick coatings; type 2, 100 mm diameter, 0.5 mm thick fused quartz wafers were used for <2 μm thick coatings; type 3, 51 mm diameter, 0.2 mm thick wafers made by Schott D263 borosilicate glass were used for 10−20 μm thick coatings. All substrates were cleaned before use by oxygen plasma in PE-200 oxygen plasma surface treatment and etching system (Plasma Etch) at 50 cm^3/min oxygen flow and 250 W radio frequency power for 10 min. Then, the substrates were primed by a 0.1% solution of DuPont VM-651 (active component is 3-aminopropyltriethoxysilane) in deionized water. The puddle of the primer stood on a substrate for 20 s. The substrate was spin dried for 60 s at 3000 rpm. The thickness of the priming

*Corresponding authors. E-mail: efremov@cae.wisc.edu and fytas@mpip-mainz.mpg.de.

Published on Web 01/14/2010

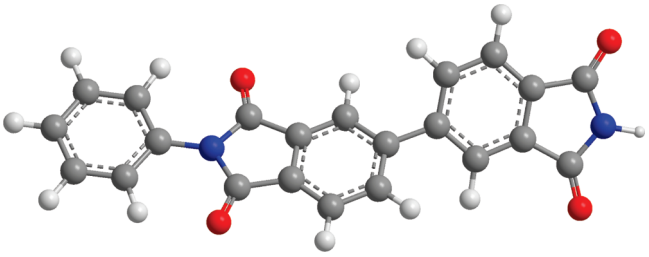

Figure 1. Chemical structure of BPDA-PDA polyimide.

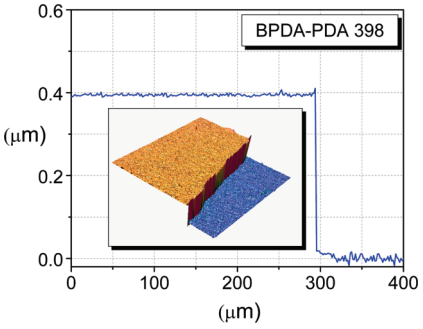

Figure 2. Scanning confocal microscope (Nanofocus AG μSurf) image showing thickness measurement for 398 nm thick polyimide film. The inset demonstrates the 3D color representation of the step profile.

layer was estimated by ellipsometry using simple method and assumptions given elsewhere.[29] Three-wavelength nulling ellipsometer AutoElII-NIR-3 (Rudolph Technologies) was used. Measured thickness value of 1.6 nm was in good agreement with literature[29] data 1.5 to 2.9 nm.

Poly(biphenyl dianhydride-*p*-phenylenediamine) (BPDA-PDA) polyimide films (see chemical structure in Figure 1) were applied on the primed side of the slides and wafers by spin coating at 1000−3000 rpm for 60 s. Both DuPont PI-2610 polyamic acid precursor and its solutions in *N*-methyl-2-pirrolidone were used. The diluted precursor with concentrations ranging from 40% and above was used for the thinnest coatings (< 1 μm thick). Neat precursor was used for the fabrication of thicker coatings. Immediately after coating, the slides/wafers were soft-baked at 130 °C for 90 s on a hot plate. To obtain thick (10−20 μm) films, we used the multiple-coating technique after soft-bake, the spin-coating was repeated. The final curing was done in a vacuum oven at 350 °C for 24 h; the ramp rate was 1 °C/min.

Sample Thickness Measurement. Accurate determination of the coating thicknesses was very important for this study. The film thicknesses were obtained by scanning confocal microscope (Nanofocus AG μSurf) equipped with a Nipkow disk, which directly measures the depth of a scratch on the films made by a sharp needle tip (illustrated in Figure 2). The mean thicknesses were computed by averaging over the whole sampled area. Additionally, the thickness of polyimide layers was verified by two methods. In the first method, the thickness was measured by reflectometry on silicon wafers coated under the same conditions as the glass slides. Filmetrics F20 reflectometer (spectral range 450−900 nm) was used, and thicknesses were measured at three points for each sample. The second method was weighting of coated wafer on a sensitive balance (Mettler-Toledo XS105 DualRange, 0.01 mg resolution) and computing the thickness by obvious geometric considerations. The density of the polyimide film used was 1.40 g/cm^3.[30] Reflectometry measurements require an external parameter−refractive index spectrum for the used range of wavelengths; coating of silicon surface can yield slightly different coating thickness. Weighting results can be biased by the nonuniformity of film thickness, especially on the wafer edges; the accuracy of the measurement rapidly decreases with film thickness. Because of these reasons, the thicknesses measured by the confocal microscope are considered to be primary values, whereas results of reflectometry and weighting are used as controls.

Brillouin Light Scattering Spectroscopy. The detailed description of the BLS setup used in this study is given in a previous publication.[31] In brief, the system is based on a high-resolution six-pass tandem Fabry−Perot interferometer and equipped with a green (λ = 532 nm) Nd/YAG laser and precision goniometer. The intensity of inelastically scattered light is recorded as a function of Brillouin frequency shift, f. Resulting Brillouin spectra are recorded in the 1−100 GHz hypersonic frequency range. A spectrum is characterized by a scattering wavevector, q, of the corresponding propagating phonon excitation, which depends on the scattering geometry. It is defined as the difference between the wave vectors of the incident laser beam (k_i) and the scattered light (k_s)

$$q = k_i - k_s \tag{1}$$

$k = 2\pi n/\lambda$, where n is the refractive index. The wavevector q is fixed for a given spectrum and the frequency shift, f, of a spectral mode in a Brillouin spectrum relates to an acoustic wave with phase velocity $v = 2\pi f/q$. Corresponding elastic modulus c can be expressed as

$$c = \rho v^2 \tag{2}$$

where ρ is the mass density.

The direction dependence of the elastic moduli is investigated by two scattering geometries.[13] In-plane mechanical properties are probed using transmission geometry, whereas reflection geometry provides access to out-of-plane characteristics. Assuming that the light source is always positioned in front of the flat sample, the detector in the transmission (or backscattering) arrangement is positioned on the back side of the film/substrate sandwich. The scattered light is monitored in the direction opposite to the reflected light: $\theta = 2\alpha$, where θ is the scattering angle and α is the incident angle. For an isotropic film, the wavevector q is parallel to the film surface: $q = q_{\parallel}$, where $\parallel$ index denotes the in-plane oriented component. The reflection geometry implies that both light source and detector are located on the same side in front of the sample. The monitored scattered light is codirectional to the reflected beam: $\theta = \pi - 2\alpha$, and the wavevector q is normal to the film surface: $q = q_{\perp}$, where $\perp$ index denotes the out-of-plane component. Probing elastic excitations with parallel- and perpendicular-to-the-film-surface wavevector, q, yield information about in-plane and out-of-plane elastic properties, respectively.

The longitudinal and shear moduli can be accessed separately by controlling the polarization of the light. In our BLS setup, the polarization of incident laser beam is always perpendicular (V) to the scattering plane. The polarization of the scattered light can be selected either perpendicular (V) or parallel (H) to the scattering plane. Polarized (VV) and depolarized (VH) Brillouin spectra correspond to light scattering by essentially longitudinal and solely by transverse phonons, respectively. Probing longitudinal and transverse polarizations gives access to longitudinal and shear elastic moduli, respectively.

Brillouin Light Scattering in Anisotropic (Uniaxial) Medium. The wavevector q definition (eq 1) implies that, in general, q depends on the refractive index, which can be direction-dependent. Polyimide coating in uniaxial medium has a single axis of anisotropy perpendicular to the surface plane. The uniaxial materials can also demonstrate birefringence. Birefringent materials are characterized by two refractive indices: ordinary index, n_o, and extraordinary index, n_e, for the light polarizations perpendicular and parallel to the axis of anisotropy, respectively. For other polarizations, effective index, n_{eff}, varies between n_o and n_e. Estimation of both indices for

Table 1. Scattering Wavevector, q, for Different Media, Geometries, and Polarizations

medium	polarization	geometry	
		transmission	reflection
isotropic	either longitudinal or transverse	$q_{\parallel} = 4\pi/\lambda \sin\alpha$, $q_{\perp} = 0$, $q = q_{\parallel}$	$q_{\parallel} = 0$, $q_{\perp} = 4\pi/\lambda(n^2 - \sin^2\alpha)^{1/2}$, $q = q_{\perp}$
anisotropic	longitudinal	$q_{\parallel} = 4\pi/\lambda \sin\alpha$, $q_{\perp} = 0$, $q = q_{\parallel}$	$q_{\parallel} = 0$, $q_{\perp} = 4\pi/\lambda(n_o^2 - \sin^2\alpha)^{1/2}$, $q = q_{\perp}$
	transverse	$q_{\parallel} = 4\pi/\lambda \sin\alpha$, $q_{\perp} \approx 0$, $q = q_{\parallel}$	$q_{\parallel} = 0$, $q_{\perp} = 2\pi/\lambda((n_o^2 - \sin^2\alpha)^{1/2} + (n_o^2 - (n_o^2/n_e^2)\sin^2\alpha)^{1/2})$ $q = q_{\perp}$

BPDA-PDA coating and $\lambda = 532$ nm wavelength is based on literature data.[17−20] Fitting of indices obtained for different wavelengths using Cauchy equation $n(\lambda) = A + B/\lambda^2$ gives $n_o = 1.893$ and $n_e = 1.663$. Birefringence magnitude $\Delta n = n_e - n_o$ is 0.23. Expressions for q in the geometries used in this work are derived in the Supporting Information section and listed in Table 1. Note that only transverse polarization measurements are affected by the film anisotropy. Even for transverse polarization and high BPDA-PDA birefringence, corrections for transmission geometry can be neglected, whereas corrections for reflection geometry do not exceed 2% under the reported experimental conditions. (See the Supporting Information.)

Results and Discussion. For the most of this section, we will discuss elastic properties in terms of phase sound velocities, v. The reason is that calculation of elastic moduli out of the phase velocities (eq 2) requires mass density, which has to be measured separately and (strictly speaking) as a function of film thickness, which is beyond the scope of this article. Lower indices l and t denote longitudinal and transverse polarizations, respectively. Upper indices $\parallel$ and $\perp$ denote in-plane and out-of-plane directed excitations, respectively.

Three different size effects are considered in this work. Potentially, the elastic parameters, refractive indices, or both could exhibit a thickness-dependent behavior. Besides this "material" phenomenon, there are two instrumental effects characteristic to BLS spectroscopy of thin supported films.

First, the propagation of elastic excitations strongly depends on the film thickness. For example, acoustic waves can, in principle, leak from the coating layer into the surrounding media (substrate and air), and this process escalates as the thickness of the coating decreases because the huge acoustic impedance leakage into the air is negligible. When the film size becomes comparable to the acoustic wavelength, $\lambda_A = 2\pi/q$, the dispersion relations for propagations both parallel and normal to the film surface deviate from the simple acoustic-like behavior.[32,33] Therefore, characteristic thickness h_1 for this size effect is determined by the minimal q used in our experiments, 0.006 nm^{-1}. It corresponds to $h_1 = 2\pi/(0.006\ \text{nm}^{-1}) \approx 1\ \mu$m.

Second, the standing acoustic wave effect is reported in refs 34 and 35 and described for coatings in detail elsewhere.[13] The longitudinal phonon mode in the reflection geometry widens as the coating becomes thinner. For thin enough films, the fine structure of the mode can be resolved. The structure prevents unambiguous measurement of the corresponding phase velocity. The resolution and instrumental widening of the BLS setup determines the characteristic thickness h_2 of the film where standing wave effect vanishes (in our case, $h_2 \approx 2-4\ \mu$m).

Then, BLS spectra for $h = 10-20\ \mu$m thick coatings ($h \gg h_1$ and $h \gg h_2$) are expected to demonstrate simple acoustic behavior: Brillouin shift, f, of a well-shaped mode is proportional to wavevector, q, and does not depend on film thickness. This trivial behavior is demonstrated in Figure 3 for 20 μm thick BPDA-PDA coating for all four combinations of geometry and polarization. Mechanical anisotropy is clearly seen as the difference in the slope (proportional to phase velocity) of linear $f(q)$ functions obtained for orthogonal directions for both

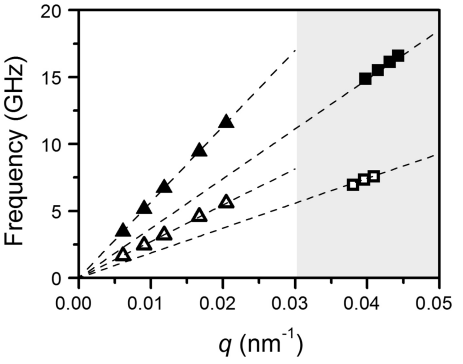

Figure 3. Mechanical anisotropy in a thick (20 μm) BPDA-PDA film. Acoustic phonons propagating with longitudinal (solid symbols) and transverse (open symbols) polarization parallel (triangles) and normal (squares) to the film surface.

Table 2. Sound Velocities for 10−20 μm Thick BPDA-PDA Coatings[a]

wave	in-plane	out-of-plane
longitudinal	$v_l^{\parallel} = 3560$ m/s, $c_{11} = 17.7$ GPa	$v_l^{\perp} = 2340$ m/s, $c_{33} = 7.67$ GPa
shear	$v_t^{\parallel} = 1710$ m/s, $c_{66} = 4.09$ GPa	$v_t^{\perp} = 1140$ m/s, $c_{44} = 1.82$ GPa

[a] Relative error is ±1.5%.

longitudinal and shear excitations. Table 2 presents sound velocities calculated from the slopes of the Figure 3 plots; the error defined as standard deviation of the data does not exceed 1.5%. Previous study of elastic properties of BPDA-PDA at hypersonic frequencies was performed by ISTS technique on free-standing films, reporting $v_l^{\parallel} = 3580 \pm 150$ m/s, $v_t^{\parallel} = 2050 \pm 100$ m/s, $v_l^{\perp} = 2330 \pm 100$ m/s, and $v_t^{\perp} = 1130 \pm 50$ m/s.[21] Remarkably, all velocities, except in-plane shear speed, $v_t^{\parallel}$, are in perfect agreement with our measurements. The nature of this "selective" discrepancy in $v_t^{\parallel}$ is unclear. Using characteristics of thick BPDA-PDA coatings as a starting point, we can address potential thickness-dependent elastic behavior by probing thinner films, where instrumental size effects are significant.

The fine structure of out-of-plane longitudinal acoustic mode detected in submicrometer coatings offers an excellent opportunity to trace the size dependence of the corresponding elastic modulus. As shown in Figure 4 (left spectra), the BLS spectra of $<2\ \mu$m films obtained for reflection geometry and longitudinal polarization develop a fine structure because of the presence of standing acoustic excitations normal to the film. The experimental line shape is represented by the sum of up to five Lorentzian lines centered at frequencies $f_m = (2m + 1)v_l^{\perp}/4h$, where m is an integer.[13] The standing wave nature of these excitations is further verified by varying q and keeping film thickness fixed. In this test, the localized modes have the same Brillouin shift regardless of q, whereas the longitudinal phonon mode envelope shifts up in frequency as q increases, as demonstrated in the right spectra of Figure 4.

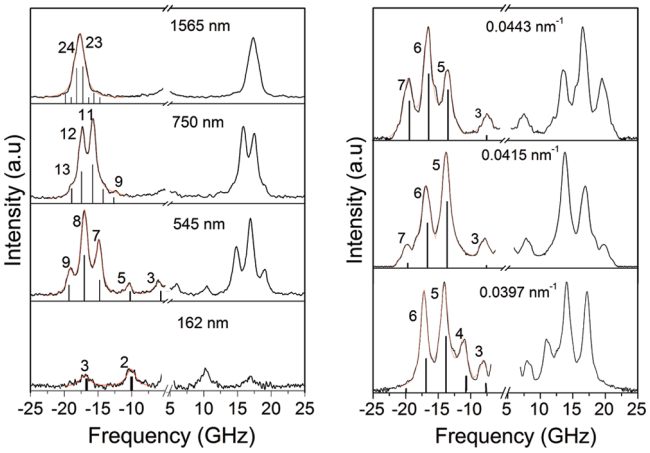

Figure 4. Thickness dependence of the out-of-plane longitudinal elastic excitations. BLS spectra are shown for the BPDA-PDA coatings with four different thicknesses ranging from 162 to 1565 nm (left panel) at a scattering angle $\theta = 150°$ ($q_\perp = 0.0443$ nm^{-1}) and for the film with $h =$ 380 nm at $\theta = 150$, 90, and 60° (right panel). The corresponding $q_\perp$ values are indicated in the plot. The spectra are well represented (red solid lines in the Stokes side) by up to five Lorentzian lines. The integers denote the vibration order, m, and the vertical lines represent the computed amplitudes of the observed modes.[13]

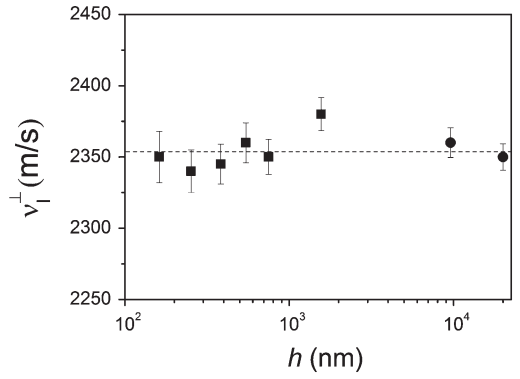

Figure 5. Dependence of out-of-plane longitudinal phase velocity, $v_l^\perp$, on thickness measured by two methods: using Brillouin shift of the propagating acoustic mode (●, 10−20 μm films) and using fine structure spacing (■, <2 μm thick films).

The frequency interval Δf between adjacent resonance modes is a function of phase velocity and film thickness, $\Delta f = v_l^\perp/2h$, and can be used to compute the out-of-plane longitudinal sound velocity independently. Figure 5 summarizes $v_l^\perp$ obtained both from fine structure spacing (less than 2 μm thick films) and from Brillouin shift of the propagation phonon mode (10−20 μm thick coatings). The $v_l^\perp$ data demonstrate no size dependence in studied thickness interval 0.16−20 μm. Excellent agreement (within ±1.5% experimental error) between $v_l^\perp$ values obtained by two methods confirm the sufficient accuracy of two used parameters: film thickness measured by confocal microscopy and ordinary index of refraction found from literature. As a practical outcome, the combination of these two methods can be used to determine one of the two listed parameters, if the other is known (under supposition that the size effect for $v_l^\perp$ is either negligible or predictable). The fine structure is found for longitudinal acoustic mode only. The reasons for depolarized BLS spectra to exhibit no standing wave effect remain unclear. One of the possible explanations is that the scattering by shear waves is significantly less intense than the signal from longitudinal phonons, and thus low signal-to-noise ratio may prevent observing the transverse mode splitting.

Another way to check the independence of elastic properties on thickness is the analysis of dispersion relations, as

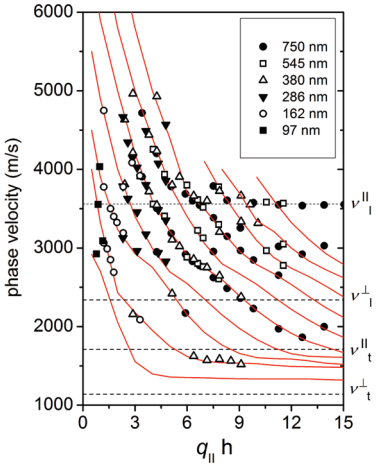

Figure 6. Dispersion diagram of the in-plane elastic excitations in supported BPDA-PDA films. The plot contains data for six different thicknesses in the 0.1 to 0.75 μm range and for q in the 0.006 to 0.022 nm^{-1} range. Correspondence between the symbols and the thickness of coating is given in the inset legend. The red solid lines represent theoretical model with all model parameters predetermined.

demonstrated for polyimide free-standing films studied by ISTS technique.[8] Six BPDA-PDA coatings with thickness in the 0.1 to 0.75 μm range (less than h_1 characteristic size) are examined in the transmission geometry, and observed modes are combined into the dispersion diagram shown in Figure 6. The data are modeled by the calculation procedure previously described.[7] The probed wave guide modes possess mixed polarization; that is, they have displacement fields in the sagittal plane. As a result, their phase velocities are functions of both the in-plane and out-of-plane intrinsic shear and longitudinal moduli. Therefore, for the particular case of BPDA-PDA polyimides, which are known to possess transverse isotropic symmetry (the in-plane mechanical properties are different from the out-of-plane ones.), the dispersion relation can be completely described by five parameters (mass density, $v_l^{||}$, $v_t^{||}$, $v_l^\perp$, and $v_t^\perp$).

All model parameters are predetermined: $v_l^{||}$, $v_t^{||}$, $v_l^\perp$, and $v_t^\perp$ values for BPDA-PDA coatings are taken from the thick film BLS measurements (Table 2); BPDA-PDA mass density, 1.40 g/cm^3;[30] v_l, v_t, and mass density of the substrate are determined beforehand. Tight correspondence of the experimental data and the model for the whole thickness range implies that elastic moduli (and mass density) determined for 10−20 μm thick films are valid down to 0.1 μm film thickness; no size effect is observed.

Thickness independence of elastic properties for BPDA-PDA polymer in the form of unsupported films is also supported by ISTS studies in the 2−10 μm thickness range.[8,21,22] No significant changes in indices of refraction and birefringence are also found for 0.4−4 μm thick BPDA-PDA coatings.[17,18] However, noticeable thickness effect in mechanical characteristics of 4−20 μm thick BPDA-PDA films is observed by so-called capacitance dilatometry technique.[23] The substantial decrease in out-of-plane modulus and increase in in-plane/out-of-plane moduli ratio as BPDA-PDA films become thinner are reported. The discrepancy can be explained by taking into account principal differences between the optical/acousto-optical methods on the one hand and the dilatometry technique on the other hand. The former methods are local and monitor processes with nano- and femtosecond characteristic times, whereas the latter technique probes the average property of the macroscopic piece of the sample (sensitive to film defects and nonuniformity) and is essentially static.

In summary, spontaneous BLS spectroscopy is used for nondestructive measurement of elastic properties of anisotropic BPDA-PDA polyimide coatings on transparent substrates. Both longitudinal and shear moduli for both in-plane and

out-of-plane directions are reported. Whereas the ISTS method has been used for similar studies of 2−10 μm thick films, this work extends the explored thickness range up to 0.1−20 μm. The elastic behavior of the supported films is shown to be size-independent in the whole thickness range investigated.

Acknowledgment. M.E. and P.F.N. thank the Global Research Collaboration (grants 2005-OCHH-985 and 2008-CHH-164), the National Science Foundation Nanoscale Science and Engineering Center at the University of Wisconsin−Madison (grant DMR0425880 and DMR0832760), and the U.S. Army Research Office through the Institute for Soldier Nanotechnologies (Contract DAAD-19-02-D-0002) for support.

Supporting Information Available: Expressions for scattering wavevector q in anisotropic film for the transmission scattering geometry. This material is available free of charge via the Internet at http://pubs.acs.org.

References and Notes

(1) Forrest, J. A.; Dalnoki-Veress, K.; Stevens, J. R.; Dutcher, J. R. Effect of free surfaces on the glass transition temperature of thin polymer films. *Phys. Rev. Lett.* **1996**, *77*, 2002–2005.
(2) Hartschuh, R.; Ding, Y.; Roh, J. H.; Kisliuk, A. P.; Sokolov, C. L.; Jones, R. L.; Hu, T. J.; Wu, W. L.; Mahorowala, A. P. Brillouin scattering studies of polymeric nanostructures. *J. Polym. Sci., Part B: Polym. Phys.* **2004**, *42*, 1106–1113.
(3) Rogers, J. A.; Maznev, A. A.; Banet, M. J.; Nelson, K. A. Optical generation and characterization of acoustic waves in thin films: fundamentals and applications. *Annu. Rev. Mater. Sci.* **2000**, *30*, 117–157.
(4) Patterson, G. D. Light-scattering from bulk polymers. *Annu. Rev. Mater. Sci.* **1983**, *13*, 219–245.
(5) Krbecek, H.; Kruger, J. K.; Pietralla, M. Poisson ratios and upper bounds of intrinsic birefringence from brillouin scattering of oriented polymers. *J. Polym. Sci., Part B: Polym. Phys.* **1993**, *31*, 1477–1485.
(6) Kumar, S. R.; Renusch, D. P.; Grimsditch, M. Effect of molecular orientation on the elastic constants of polypropylene. *Macromolecules* **2000**, *33*, 1819–1826.
(7) Cheng, W.; Sainidou, R.; Burgardt, P.; Stefanou, N.; Kiyanova, A.; Efremov, M.; Fytas, G.; Nealey, P. F. Elastic properties and glass transition of supported polymer thin films. *Macromolecules* **2007**, *40*, 7283–7290.
(8) Cocson, J. K.; Hau, C. S.; Lee, P. M.; Poon, C. C.; Zhong, A. H.; Rogers, J. A.; Nelson, K. A. Transverse isotropic elastic moduli and in-plane thermal diffusivity in silicon-supported thin-films of a photosensitive polyimide measured using impulsive stimulated thermal scattering. *Polymer* **1995**, *36*, 4069–4075.
(9) Dhar, L.; Rogers, J. A.; Nelson, K. A.; Trusell, F. Moduli determination in polyimide film bilayer systems: prospects for depth profiling using impulsive stimulated thermal scattering. *J. Appl. Phys.* **1995**, *77*, 4431–4444.
(10) Sun, L.; Dutcher, J. R.; Giovannini, L.; Nizzoli, F.; Stevens, J. R. Elastic and elasto-optic properties of thin films of poly(styrene) spin-coated onto Si(001). *J. Appl. Phys.* **1994**, *75*, 7482–7488.
(11) Forrest, J. A.; Rowat, A. C.; Dalnoki-Veress, K.; Stevens, J. R.; Dutcher, J. R. Brillouin light scattering studies of the mechanical properties of polystyrene/polyisoprene multilayered thin films. *J. Polym. Sci., Part B: Polym. Phys.* **1996**, *34*, 3009–3016.
(12) Dil, J. G.; van Hijningen, N. C. J. A.; van Dorst, F.; Aarts, R. M. Tandem multipass Fabry-Perot interferometer for brillouin scattering. *Appl. Opt.* **1981**, *20*, 1374–1381.
(13) Gomopoulos, N.; Cheng, W.; Efremov, M.; Nealey, P. F.; Fytas, G. Out-of-plane longitudinal elastic modulus of supported polymer thin films. *Macromolecules* **2009**, *42*, 7164–7167.
(14) Hartschuh, R. D.; Kisliuk, A.; Novikov, V.; Sokolov, A. P.; Heyliger, P. R.; Flannery, C. M.; Johnson, W. L.; Soles, S. L.; Wu, W.-L. Acoustic modes and elastic properties of polymeric nanostructures. *Appl. Phys. Lett.* **2005**, *87*, 173121.
(15) Bandhu, R. S.; Zhang, X.; Sooryakumar, R.; Bussmann, K. Acoustic vibrations in free-standing double layer membranes. *Phys. Rev. B* **2004**, *70*, 075409.
(16) Hinrichs, K.; Eichhorn, J. Combined infrared (IR) and visible (VIS) spectroscopic ellipsometry (SE) study of thin polymer layers. *Spectrosc. Europe* **2007**, *19*, 11–14.
(17) Herminghaus, S.; Boese, D.; Yoon, D. Y.; Smith, B. A. Large anisotropy in optical properties of thin polyimide films of poly(*p*-phenylene biphenyltetracarboximide). *Appl. Phys. Lett.* **1991**, *59*, 1043–1045.
(18) Diao, J.; Hess, D. W. Through-plane uniformity of optical anisotropy in spin-coated biphenyl dianhydride-*p*-phenylenediamine films. *Thin Solid Films* **2005**, *483*, 226–231.
(19) Hinrichs, K.; Tsankov, D.; Korte, E. H.; Röseler, A.; Sahre, K.; Eichhorn, K. J. Comparative study of an anisotropic polymer layer by infrared spectroscopic techniques. *Appl. Spectrosc.* **2002**, *56*, 737–743.
(20) Sahre, K.; Eichhorn, K.-J.; Simon, F.; Pleul, D.; Janke, A.; Gerlach, G. Characterization of ion-beam modified polyimide layers. *Surf. Coat. Technol.* **2001**, *139*, 257–264.
(21) Rogers, J. A.; Dhar, L.; Nelson, K. A. Noncontact determination of transverse isotropic elastic moduli in polyimide thin films using a laser-based ultrasonic method. *Appl. Phys. Lett.* **1994**, *65*, 312–314.
(22) Rogers, J. A.; Yang, Y.; Nelson, K. A. Elastic modulus and inplane thermal diffusivity measurements in thin polyimide films using symmetry-selective real-time impulsive stimulated thermal scattering. *Appl. Phys. A: Mater. Sci. Process.* **1994**, *58*, 523–534.
(23) Liou, H. C.; Willecke, R.; Ho, P. S. Study of out-of-plane elastic properties of PMDA-ODA and BPDA-PDA polyimide thin films. *Thin Solid Films* **1998**, *323*, 203–208.
(24) Kurabayashi, K.; Goodson, K. E. Impact of molecular orientation on thermal conduction in spin-coated polyimide films. *J. Appl. Phys.* **1999**, *86*, 1925–1931.
(25) Morikawa, J.; Hashimoto, T. Thermal diffusivity of aromatic polyimide thin films by temperature wave analysis. *J. Appl. Phys.* **2009**, *105*, 113506.
(26) Wilson, D. *Polyimide*; Plenum Press: New York, 1984, p 767−782.
(27) Senturia, S. D. Polyimides in Microelectronics; Boweden, J., Turner, S. R., Eds.; ACS Symposium Series 428; American Chemical Society: Washington, D.C., 1987.
(28) Yokota, R. *Aerospace Materials in Proceedings of 1st Oxford Kobe Materials*; St. Catherine's College, Kobe, 1998.
(29) Howarter, J. A.; Youngblood, J. P. Optimization of silica silanization by 3-aminopropyltriethoxysilane. *Langmuir* **2006**, *22*, 11142–11147.
(30) PI-2600 Series−Low Stress Polyimides, HD MicroSystems, 250 Cheesequake Road, Parlin, NJ 08859-1241. www.hdmicrosystems.com.
(31) Penciu, R. S.; Kriegs, H.; Petekidis, G.; Fytas, G.; Economou, E. N. Phonons in colloidal systems. *J. Chem. Phys.* **2003**, *118*, 5224–5240.
(32) Farnell, G. W.; Adler, E. L. In *Elastic Wave Propagation in Thin Layers: In Physical Acoustics*; Mason, W. P, Thurston, R. N, Eds.; Vol. 9, 1972.
(33) Auld, B. A. *Acoustic Fields and Waves in Solids*, 2nd ed.; Krieger: Malabar, FL, 1990; Vol. *II*.
(34) Sandercock, J. R. Structure in brillouin spectra of thin films. *Phys. Rev. Lett.* **1972**, *29*, 1735.
(35) Sandercock, J. R. Brillouin scattering measurements on silicon and germanium. *Phys. Rev. Lett.* **1972**, *28*, 237.